Hindawi
Mathematical Problems in Engineering
Volume 2022, Article ID 2752443, 9 pages
https://doi.org/10.1155/2022/2752443

Research Article

An Internet of Things (IoT) Based Image Process Screening to Prevent COVID-19 in Public Gatherings

Suhail H. Serbaya

Department of Industrial Engineering, Faculty of Engineering, King Abdulaziz University, Jeddah 21589, Saudi Arabia

Correspondence should be addressed to Suhail H. Serbaya; sserbaya@kau.edu.sa

Received 12 August 2022; Revised 10 September 2022; Accepted 24 September 2022; Published 9 November 2022

Academic Editor: Savita Gupta

Copyright © 2022 Suhail H. Serbaya. This is an open access article distributed under the Creative Commons Attribution License, which permits unrestricted use, distribution, and reproduction in any medium, provided the original work is properly cited.

The global community is now coping with such a significant issue as the Covid-19 virus, public gatherings are experiencing certain restrictions in order to stop the virus from spreading further. The issue takes on a bigger significance during religious pilgrimages such as the Hajj and the Umrah, when tens of thousands, if not hundreds of thousands, of people gather in holy cities to participate in religious rituals. During such a time period, it is quite difficult to single out an infected person from among the big crowd that is there. The current screening approach only includes a single element of identity, which means that there is a possibility that the screening process may fail because there will not be enough identification. The use of thermal imaging provides a higher level of accuracy when compared to more conventional ways of testing for viral infections in the detection of these symptoms in crowded locations. The primary method that is utilised to determine whether or not a person is infected with the virus is an image processing algorithm that is built in MATLAB. The first step in the process of acquiring an image is to divide the video that is being captured into individual frames. Following this step, the frames that have been focussed are processed in a number of ways. The temperature of a person's body may be estimated by taking a thermal image and then using the RGB separation feature on it. In order to categorise and sort the data, the k-means approach was used as part of the segmentation operation. In addition to eliminating the skin frequency, it also gets rid of the background noise, which often has a higher frequency than the skin frequency. The Viola–Jones technique, which may be used to identify the person's breathing rate, can be used to locate the end of a person's nose, specifically the tip of the nose. The Cascaded Adaboost Classifier is an option that may be used to finish the classification process after the operation has been completed. The suggested method has an accuracy rate of 89.23 percent and a simulation period of around 60 seconds, which guarantees the safety of huge groups of people's public health.

1. Introduction

It is necessary to shorten the duration of the blockchain in order to increase the pace at which the pandemic sickness is spread [1]. According to the Globe Health Organization, fever is one of the most prominent symptoms of the coronavirus and has been seen in a variety of places throughout the world to interrupt the cycle of transmission of the virus. Individuals are screened with the use of infrared thermography in a number of contexts, including airports, railway stations, and other public venues [2, 3]. Infrared thermography is one of the most efficient methods available for identifying fever symptoms in passengers. Despite the fact that IRT is a very powerful method, it is not going to be enough in all circumstances. The IRT technique could not provide accurate results when used to patients who were on antipyretic medication [3]. The results of the IRT-based screening technique indicate that there are problems in the detection process [4]. The findings vary from 35 percent to 66 percent, which indicates that there is a significant range. It is strongly recommended that employees be checked utilising a wide range of symptoms in order to minimise this drawback. As a result of changes in the respiratory system, COVID-19 causes multiple changes in vital signs, the most notable of which are a slowing of the heart rate and a raising of the temperature of the body. A thermal surveillance camera is employed internally to check for the existence of these important signs [5].

Figure 1 demonstrates the process of contactless screening that will be used for the proposed task. During the

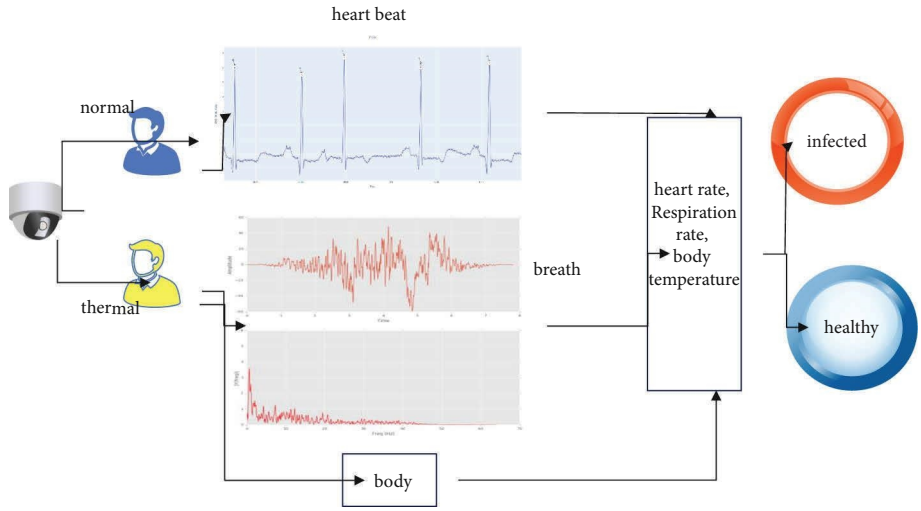

Figure 1: Contactless vital sign measurement systems for symptoms screening.

screening process, the RGB thermal camera observes the variation in the quantity of light that is being emitted by the subject in order to calculate the amount of blood pulse [6]. The light absorption factor in the recommended task, which was assessed using the model derived from the Covid-19 patient, was responsible for the various changes that can be seen in the employee's face, which can be seen in the photo that was taken, which includes the employee's facial region. [7] The inquiry that has been proposed requires that there be no human subjects or participants involved in order to identify a number of symptoms that are associated with the virus. Utilizing the RGB channel of the image input, the work that has been finished mostly concentrated on distinguishing between the blood pulse and the breathing rate [8].

When looking at ways to reduce death rates over the long term, placing a greater emphasis on early therapies may prove to be beneficial. Patients who are in critical condition are obliged to make use of ventilators and to be admitted to an intensive care unit (ICU) as soon as possible [9]. Since COVID-19 patients often arrive to the hospital after the illness is already in a more advanced state, medical professionals are frequently unable to provide an accurate prognosis for these patients at the time of their admission. It is possible that the progression of COVID-19 will occasionally take unexpected turns. One example of this is when the health of a patient who appeared to be in stable condition suddenly deteriorates to a critical stage. This is something that can take even the most experienced physicians by surprise. Artificial Intelligence (AI) models have the potential to be effective tools in improving clinical prediction because they are capable of finding complex patterns in large datasets, which is a feature that the human brain is not capable of achieving on its own. This is one of the reasons why AI models have the potential to be effective tools in improving clinical prediction. In the battle against COVID-19, technologies using artificial intelligence have been applied on a variety of scales, ranging from epidemiological modelling to personalised diagnosis and prognostic prediction [10]. These applications of artificial intelligence include: Even though a number of different COVID-19 prognostic models have been developed, no exhaustive study has been carried out to analyse and compare the prognostic prediction capacity of noninvasive and invasive factors in the COVID-19 patient group.

In order for the researcher to accomplish these three goals, the first step is to collect routine clinical data from patients on the first day of their admission. The second step is to determine whether noninvasive patient characteristics can predict the COVID-19 mortality outcome. Finally, the third step is to conduct a direct comparison of the mortality prediction powers of noninvasive and invasive patient characteristics [11]. In the first instance of the aforementioned feature groups, noninvasive demographic and clinical factors were separated from invasive laboratory tests in order to facilitate an effective analysis of patient data. This was done because invasive laboratory tests required a greater level of physical access. According to the findings of many studies, the vast majority of COVID-19 patients had their first exacerbation episode between 24 and 48 hours after being admitted to the hospital [12].

A signal extraction method may be constructed from the RGB image that was used as input, which is what was used to accomplish the task of extracting the blood pulse rate. This method was employed. In order to investigate the respiration rate, we are decreasing the SNR value. In order to do this, we are relying on the signal quality index. An Excel sheet is used to compile the employee's medical history, after which it may be uploaded to a more comprehensive government database [13]. During the testing method, which takes place inside the company, there are a total of 20 people taking part: ten healthy volunteers and ten ill ones.

As the pandemic disease has become more widespread, several different approaches have been devised to combat it. Goldberg and colleagues came up with a novel approach to evaluating the levels of blood saturation by making use of a digital camera [14]. In addition to identifying position, this camera can also pick up on a person's temperature. The

image processing technique that was used in the suggested research, which was based on their initial hourglass network, is an essential component [15, 16]. They referred to it as the "Rapid Response Analysis Method," and Poh Ming and his colleagues came up with it. This method was developed to determine the rate of breathing and other vital sign readings while simultaneously recording video with RGB and using changes in the color of the skin. Martinez et al. [17] quantified the movement of the chest by using the red Dot Matrix while conducting a mobility experiment. In this particular instance, infrared imaging will be used so that the human posture estimation may be determined. It is possible to assess the radiation pattern of an object using thermal imaging technology if the person's body temperature is greater than zero degrees Celsius. Xiao, Xuan, and colleagues have developed a camera-equipped smartphone that can determine a person's respiration rate by tracking the movement of their chest and abdomen [18]. When doing this activity, the median number of errors often falls below 2 percent. Basu and colleagues developed a technique to identify changes in the rates of respiration across individuals by using thermal imaging that was based on infrared thermography [19]. He was also responsible for determining the heart rate by applying the method of continuous monitoring of the pulse. According to the results of a number of different survey investigations, it is possible to determine a person's heart rate by observing the blood circulation of that individual. On the other hand, a great number of investigations have shown that filters are applied to remove inaccuracies in the measurement of heart rate. Yan et al. made advantage of this circumstance in order to calculate a person's heart rate using a video of a red, green, and blue facial picture that was lighted by sunlight [13]. To analyse a person's heart rate using monochrome and infrared cameras, Gupta et al. developed a multi-model technique, which they reported in Science [12]. This approach was similar to the one described above. According to [16], the outputs of the experiment have a reasonable accuracy range when the procedure of guiding it is being carried out. The comprehensive research was conducted under natural conditions, and it was found that an infrared sensor could be utilised to monitor the subject's heart rate as well as their breathing rate [20]. Utilizing a dual imaging approach allows for the estimation of the blood oxygen saturation rate. It is not possible to identify the current pandemic illness based only on a single sign measurement [19]. This is due to the reasons discussed above, as well as the fact that multiple thermal screening methods are currently in use. As a result, it is of the utmost importance to devise a screening strategy that incorporates a number of distinct readings for the vital signs. In the event that an employee in the firm contracts the disease, the suggested course of action would be to bring the individual's health information that is stored in the organisation up to date.

A timely and accurate diagnosis of COVID-19 is possible because to effective screening for SARS-CoV-2, which also helps to reduce the load on healthcare delivery systems. The likelihood of infection may now be predicted using models that take into account a number of different factors simultaneously. These are intended to provide assistance to medical personnel all over the globe in the process of triaging patients, which is particularly important given the limited resources available in the healthcare sector. We developed a method based on machine learning that was taught using data from 51,831 people who were assessed (of whom 4769 were confirmed to have COVID-19). The results from the next week were included in the sample set to be examined (47,401 tested individuals of whom 3624 were confirmed to have COVID-19). Our model was able to accurately predict the outcomes of the COVID-19 test by utilising just eight binary characteristics, which were gender, age under 60 years, known contact with an infected person, the presence of five early clinical signs, and known exposure to the virus. Overall, we constructed a model that identifies instances of COVID-19 by using simple indicators that can be accessible by asking fundamental questions. This model was based on the countrywide data that was publicly disclosed by the Israeli Ministry of Health. When there are limited resources available for testing, our methodology may be utilised as one of the factors in the decision-making process to prioritise testing for COVID-19.

2. Materials and Methods

In accordance with the process that had been detailed before, a 10-fold cross-validation was carried out in order to train and tune the model using different examples from the training set [17]. These curves were produced using an algorithm that was not dependent in any way on the technique selecting criteria that were used in the building of the algorithm. When it comes to making accurate predictions, the performance of the noninvasive model seems to be on par with that of the joint model. There were determined to be no statistically significant differences between the two models after a further in-depth statistical investigation [18] discovered that there were. To determine whether or not there were statistically significant variations in the performance of the models and to test the resilience of the data [21] concerning sample sizes, a hold-out cross-validation with a percentage of 10 percent was carried out for a total of 20 iterations. This was carried out. [Cross-validation] At the end of each iteration, ten percent of the data was chosen at random and included into the process of training the model and evaluating the remaining data. The findings demonstrated that the models were insensitive to changes in the sample size, and they also revealed that there was no statistically significant difference between the invasive and noninvasive models [22]. Conclusions: test accuracy ratings for models that had joint, noninvasive, and invasive components were, respectively, 0.80 0.03, 0.77 0.04, and 0.75 0.4, with the joint model having the greatest accuracy out of the three types of models.

Infrared thermal imaging is used in conjunction with an RGB image combination to facilitate the monitoring of a subject's heart rate, respiration rate, and body temperature. Matlab software must be used in order to carry out image processing procedures, and the organization's server must be kept current and up to date with regard to the health-related

database. Both of these requirements must be satisfied. The thermal imaging camera model FLIR C2 is now being evaluated for potential use in the next research project. It has a temperature range of −14 to 302 degrees Fahrenheit and an infrared resolution of 80 × 60 (4800). In addition, it is able to function in this temperature range. The memory capacity of the camera in question is something in the neighbourhood of five hundred images at a bare minimum. The pixel resolution of the digital camera ranges from 640 × 480 all the way up to 960 × 1280, and the pace at which it can capture video is around 15 frames per second (640 × 480).

2.1. Face Detection and Breathing Rate Calculation. Because the breathing rate is calculated based on the facial region, it is vital to determine the area around the face. The RGB thermal camera is used to make the determination of the age of the worker. There are flicker cameras on the market that make use of infrared thermography to determine a person's body temperature, as well as their heart rate and breathing rate. The RGB camera was used to record the changes in haemoglobin that occurred in the facial region when blood vessels were subjected to light absorption, and the results of this experiment were acquired by the camera. During inhalation and exhalation, respectively, the flickering camera is used to determine the variation in temperature that occurs in the nasal region. After the image had been processed, the Viola–Jones method was applied to it in order to isolate the facial area from the rest of the picture. K-means segmentation is used in order to complete the task of segmenting the region around the nose. An rise in a person's fever, abnormalities in their breathing rate, and irregularities in their heart rate are all signs that a person is sick, and these symptoms may be used to identify infected people. The research that has been conducted shows that there is a clear divide between those working in the industry who are healthy and those who are afflicted with sickness. Following the implementation of the Viola–Jones technique, the face detection procedure is carried out in the phases that are listed as follows.

Step 1. The attributes of the bigger window size are gathered as a sliding phase in the process, while the smaller window size is gathered as a subwindow.

By moving the sliding window in both the vertical and horizontal orientations in both directions, it is possible to compare the line and edge properties of the photo that was entered by the user.

When the sliding window has reached its maximum position in step three, the corresponding subwindow may be deleted.

Figure 2 depicts the technique that has been discussed.

In Figure 2, the Haar, edge, and line characteristics of the input pictures are represented by the letters F1, F2, and F3. Calculating the respiration rate begins with the collection of data from the input picture via the use of the K-means segmentation technique. It is possible to compute the breath rate by comparing changes in the RGB area between two frames and the nasal region segregated using the K-means

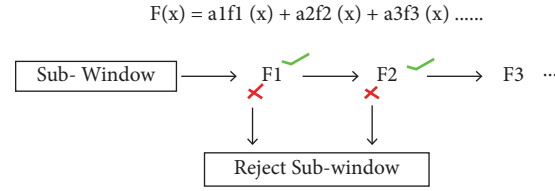

Figure 2: Viola–Jones algorithm.

algorithm. The following is the equation that was used to estimate the rate of breathing. Thermal image segmentation may be used to separate the parts of the nose and mouth that are visible. When the sampled thermal image u is transformed into a two-dimensional magnitude map of thermal-gradient u by the boundary detection technique, the breathing area will be divided into two halves. The breathing region will be divided by the boundary detection method.

$$he\,\Phi(x,y) = \sqrt{\left(\frac{\partial u(x,y)}{\partial x}\right) + \left(\frac{\partial u(x,y)}{\partial y}\right)}, \tag{1}$$

x and y parameters represent the coordinates of the x-y plane in the image matrix. The heat exchange during inhalation and exhalation determines the proposed breathing pattern of the victim. Consecutive frames are selected, and the average value of the spatial thermal distribution calculated for each frame.

$$v(t) = \int_0^{Tmin} S(t)dt \approx \sum_i^t \sum_j^t T\delta(t) - u\hat{i}j(t), \tag{2}$$

where $v(t)$ determines the thermal value of the nose region in the cross-sectional view whereas the temperature T, $u\hat{i}j$ represents the temperature with the absolute value in the tracked area, and $T\delta$ indicates the upper boundary level to the inner volume of the segmented thermal image that is above the temporal moving value ($n = 2$) in the spatial domain. The spatial temperature represents the global thermal changes within the image. If the K-means algorithm loses the nose region's data, $T\delta$ will element the present frame and move on to the next frame with the bounding box region.

2.2. Image Processing Techniques to Detect Vital Signs. Figure 3 depicts the method used by the Viola–Jones approach to recognize a facial picture in a photograph. It is the Viola–Jones algorithm that is used to recognize faces in images. The letter k indicates that segmentation was performed in order to separate the tip of the nose. In order to retrieve the single feature of the picture, the pixel value of the nose area is computed and used. The respiration rate may be calculated using the pixel attributes of each frame, which can be found in a calculator. A Fast Fourier transform is used to a respiratory signal in order to determine the rate at which the person is breathing. Using the total number of pixels (px) in the segmented picture and the original image (py), the segmentation procedure is evaluated for its proximity to the original image.

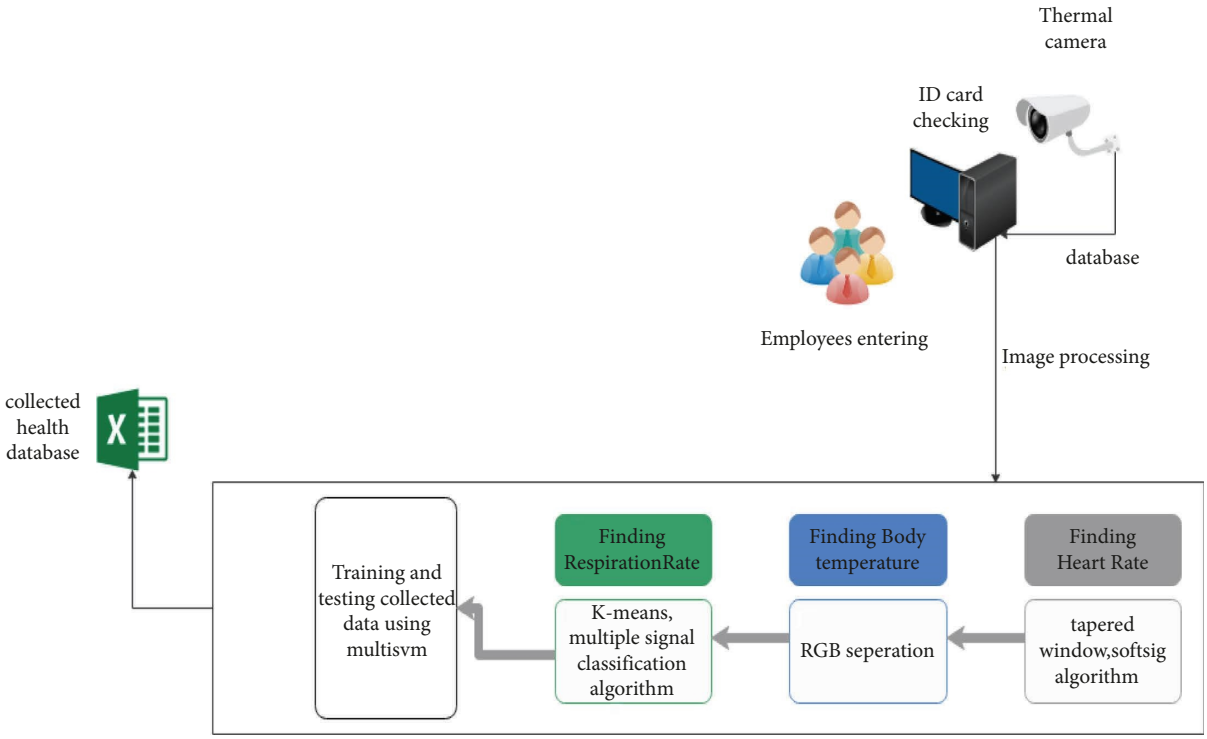

Figure 3: Block diagram of the proposed work.

$$\text{Input Image Closed Percentage} = \frac{A1}{A2} * 100. \tag{3}$$

During the inhaling and exhalation processes, the color of the tip of the nasal area changes from red to blue to green. Changing the RGB region will result in corresponding changes in the pixel area. The Viola–Jones method is used to recognize the face area in a thermal picture captured with a thermal camera.

Figure 4 shows the nose area being segmented using the K-means segmentation method, which is achieved by the fusion of RGB and thermal imaging images. The respiration signals are retrieved from the identified locations with the use of pixels included within the pictures, which are used to extract the signals. The following equation may be used to calculate the mean temperature and the height of the segmented area.

$$x\text{mean}(t) = \frac{1}{mn}\sum_{x=0}^{m=1}\sum_{y=0}^{n=1} I(x, y, t) = I(x, y, t). \tag{4}$$

The respiration signals are included in the functions $x$mean(t) and $x$min(t). With respect to the segmented image, I (x, y, t) represent the pixel range in terms of temperature with the image coordinates of (x, y) in the segmented image and time t, m indicates the extracted signals, which are: $x$mean nose(t), $x$min nose(t), $x$mean (t), and $x$min nose(t) (t). Respiration signals are selected based on their temperature traces in the three different channels of the input picture, which are split into three groups. The frequency of the input image's respiration is the most important element in determining the rate at which it is breathing.

2.3. RGB Processing for HR Estimation Using Tapered Window. To detect the Region of Interest facial a general window function is used which is nothing but a Tapered window (Figure 4(b)). The edge area is impacted by the latency caused by the face tracker in the facial Region of Interest, which is visible in the edge region. Instead, the center of the Region of Interest may be used to create steady tracking of the face skin, which is more accurate. To reduce the amount of noise lifted by the face tracking, we obtained a tapered window to a weighted Region of Interest and applied it to the facial tracking data.

$$\%\ \text{taper}(i) = \{i = 0, 1, 2, \ldots m - 1 i = n - m, \ldots . n \text{ otherwise}\}. \tag{5}$$

By using the divergence between absorption of RGB and signal, the purpose of signal reconstruction is to determine the identity of a reconstruction vector $V = r, g$, and b in order to recover the signal from the heartbeat using the absorption of RGB and signal. It is necessary to employ three RGB channels in order to optimize a linear function for enhancing the SNR value while reconstructing a BVP signal. The pulse reflection strength, according to earlier study, is referred to as the link in $G > B > R$, which categorizes the RGB channels based on their intensity levels. With the help of this link, the reconstruction of the signal may be represented as follows:

$$y(t) = V_r X_r(t) + V_g X_g(t) + V_b X_b(t). \tag{6}$$

Vector reconstruction is represented by the variables vr, vg and vb. Unlike this strategy, which is based on the Softsig method, we enhance the process of identifying the

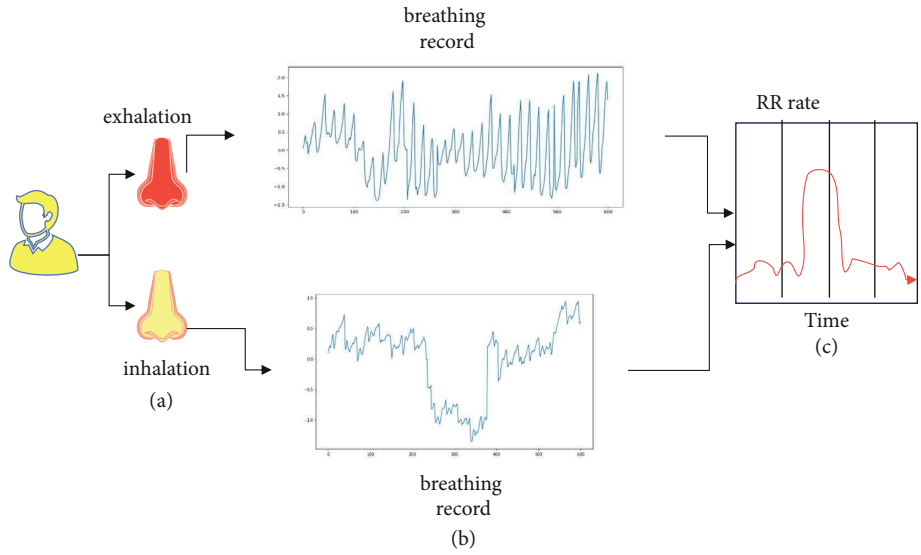

Figure 4: Block diagram of signal processing for respiration rate (RR) estimation. (a) Segmented Region. (b) Time-series extracted from RGB signal. (c) Power spectrum.

procedure for vector V. We picked V in order to increase the kurtosis of the spectra in the Heart Rate range of [0.87–4.97 Hz] in order to get a better signal of the heartbeat. Finally, the MUSIC system was established in order to interpret Heart Rate and Respiration Rate data in a short period of time. A high-resolution frequency estimate of Heart Rate and Respiration Rate is possible with this approach, which allows for a better comprehension of the frequency. The current technique for monitoring respiration using an IRT is based on the temperature change of the nasal passages.

3. Results and Discussion

As previously stated, the primary frequency noise component is included in a raw trace color of RGB and is distinguishable by their spectra, as the pulse oximeter gives 1.83 Hz during the measurement of Heart Rate, which is considered the ground truth. By using the suggested approach, it is possible to detect an evident peak in the component of Heart Rate frequencies shown in Figure 5. The benefits of having a planned Heart Rate evaluation are shown in this example.

For example, as shown in Figure 6, the raw green trace, which utilizes FFT and just one green channel, is compared to the suggested technique for evaluating signal reconstruction and the tapered window, which is shown by the dotted line in Figure 5. If you have an RGB camera and want to monitor the heart rate of a person, you may use the same fundamental method as the green trace. A pulse oximeter and an electrocardiogram are used to assess the heart rate of the patient. The heart rates of 128 pairs of individuals were measured four times 15 seconds apart next to healthy control participants. The subjects comprised 41 patients with flulike symptoms and 22 healthy control subjects in the study, for a total of 128 pairs of subjects.

Figure 5(a) depicts the green trace process of the scatter plot, with the Pearson correlation coefficient (R) at the time of analysis being 0.48 (green trace process). The proposed Bland–Altman strategy, shown in Figure 5(b), makes use of a variety of approaches, including signal reconstruction, Music, and tapered window techniques, among others. The 95 percent limits of agreement vary from −10.7 to 12.9 bpm (standard deviation = 5.89), with a root mean square error of 5.97. The 95 percent limits of agreement range from −10.7 to 12.9 bpm (standard deviation = 5.89). There is a mean of −10.7 between the 95 percent bounds of agreement. This method's scatter plot is shown in Figure 7(d); the Pearson correlation coefficient for this specific technique was 0.91, which indicates that it is very effective. The experimental findings reveal that the proposed strategy has the potential to lower the 95 percent limits of agreement from [23.9, 33.8] bpm to [10.7, 12.9] bpm, which is a statistically significant decrease. As a result of the clinic environment serving as a mimic of a real-world scenario, patients suffering from flulike disease (red circle) fared far better than the general population.

It was in December of the year 2019 that this pandemic crisis started in China, and it has since spread around the world. By the end of March 2020, this virus would have infected more than 110 countries all over the globe, according to estimates. Coughing, high fever, and irregularities in the body's physiology are among of the most visible signs of the dress pandemic illness, which has spread over the world. By using new technologies, the proposed research was able to enhance the multiscreening of the infection's vital signs. It is designed for use mainly in the screening of interpretive signs using a contactless technique, which is the primary application of the proposed technology. During this endeavor, data from both healthy and sick people will be collected and trained. There is a prototype model proposed in this study that is more compatible and accurate than the present model.

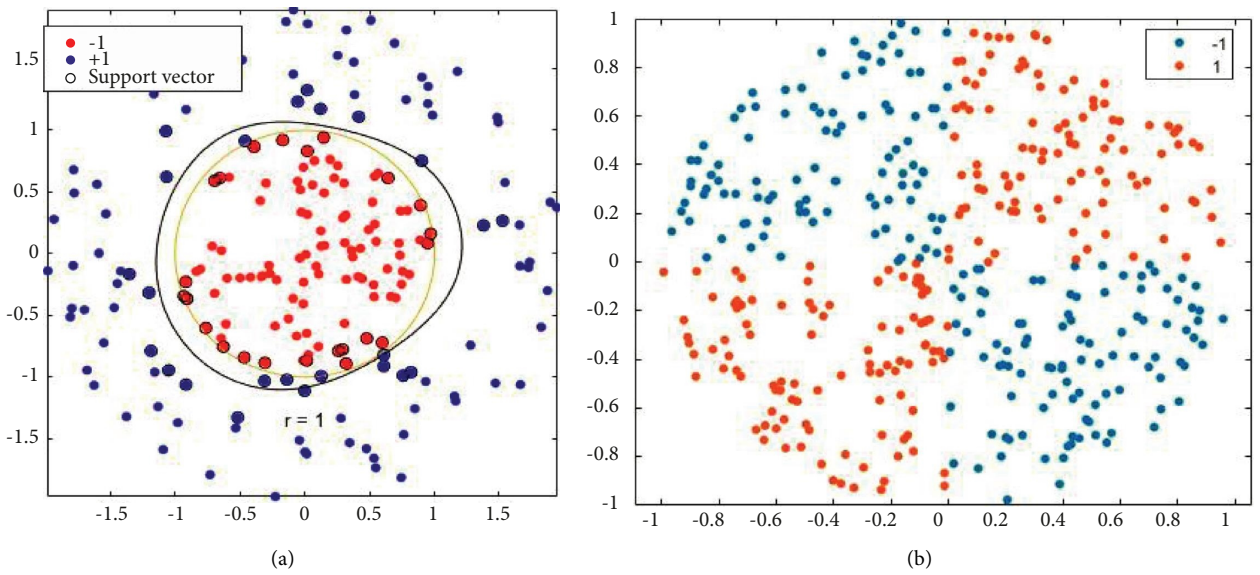

Figure 5: (a) Classifier training region. (b) Classifier tested region.

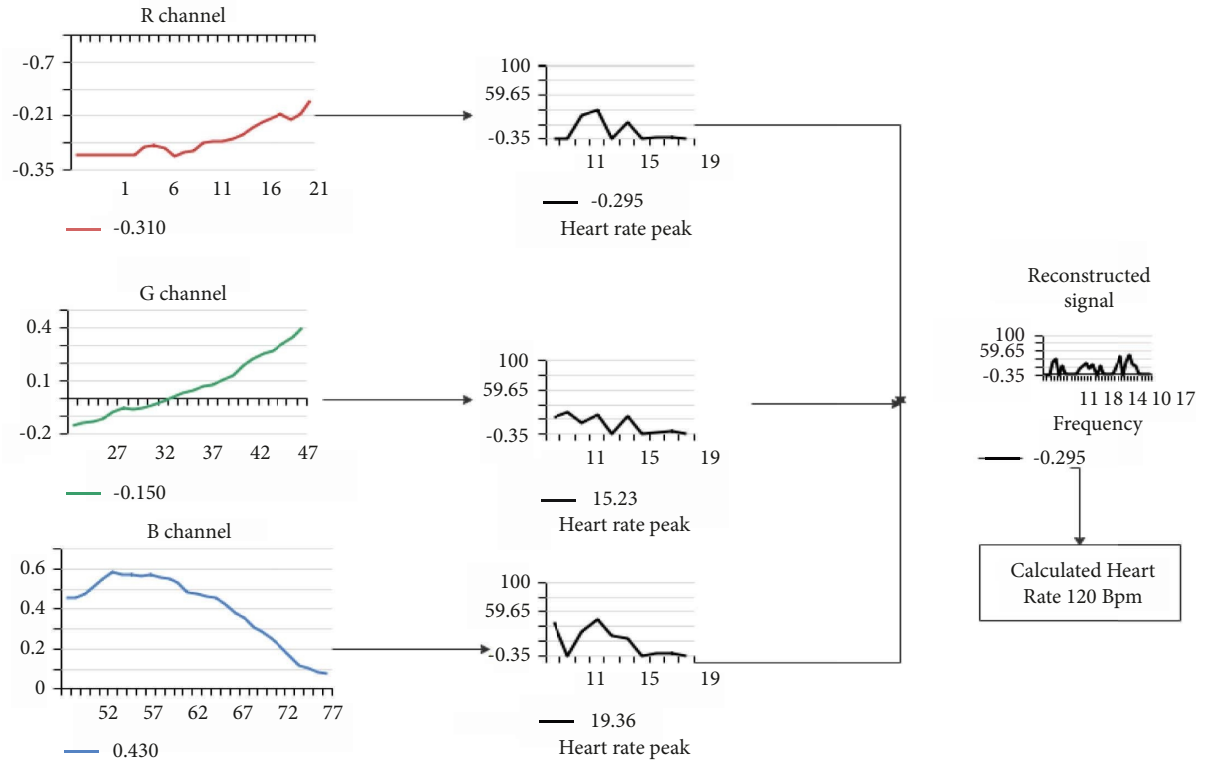

Figure 6: Reconstructed signal.

Techniques such as the tapered window method, k-means segmentation, and support vector machine classification are among those used in the suggested investigation. The Viola–Jones method takes as input a thermal image and extracts a face area from the face region using the face region as input. [10.12, 12.32] beats per minute, [2.123, 3.86] beats per minute, and temperature: [0.687, 2.84] degrees Celsius, the suggested study reveals the similarity between the heart rate of the infected individual and the reference device [23]. Using the suggested study, it will be possible to show the similarity between the heart rate of the infected individual and the reference device. The stability and reliability of our framework in terms of its ability to provide vital signs has been greatly enhanced.

The classifier predicts the output class as an infected or healthy person and writes up in the XL sheet as shown in

1	class1	[1]
2	class2	[0]
3	class1	[1]
4	class1	[1]
5	class1	[1]
6	class2	[0]
7	class2	[0]
8	class1	[1]
9	class2	[0]
10	class1	[1]
11	class2	[0]
12	class2	[0]
13	class2	[0]
14	class1	[1]

Figure 7: Classifier result.

Table 1: Calculated metrics from classifiers.

	TP	TN	FP	FN
Actual_class1	10	0	0	90
Actual_class2	25	0	0	75

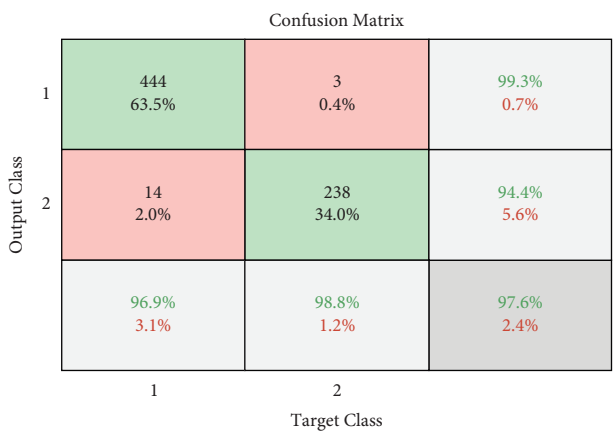

Figure 8: Confusion matrix.

Figure 7. The predicted class gives the binary range where 0 as a healthy person and 1 as an infected person.

Table 1 represents the Performance metrics calculated from the predicted class which decides the accuracy range of the classification process.

As shown in Figure 8, the confusion matrix depicts the training accuracy of the gathered characteristics. The planned job will be submitted to a screening process that will include the affected individual inside the business as well as personnel in familiar locations.

4. Conclusion

The global community has been put in the position of dealing with a myriad of problems ever since the COVID-19 made its debut not too long ago. Keeping the propagation of viruses under control in crowded surroundings is one of the challenges that presents one of the greatest opportunities for frustration and failure. By monitoring a variety of measurements of the patients' vital signs, the researcher in this study aimed to identify individuals who were infected. Using real-time measurements, a brand-new system has been constructed, and it has the capacity to evaluate a huge number of essential sizes in real time. Real-time measurements have been used. A wide range of sign measures that are based on thermal imaging need the use of thermal image processing methods, and it is necessary to have these techniques available. The k-means methodology, which was used throughout the whole of the segmentation process, was utilised in order to segment the data. Particularly in this study, techniques of image processing were employed to amplify the minute temperature variations generated by facial-skin blood flow. The heart rate was computed based on the amplified temperature signal that was applied, and the results were presented in this work. The Viola–Jones technique is used in order to identify the tip of the nose, which is then utilised in the subsequent calculation of the individual's breathing rate based on the tip of the nose. At the end of the procedure, the Cascaded Adaboost Classifier is used to complete the classification process that was started earlier in the procedure. The findings are recorded in a database sheet that is maintained on a consistent basis and include information on the health of the staff members. The accuracy rate of categorization reveals that 82.25 percent of the classifications are accurate, while only 81.05 percent of the classifications are inaccurate. This ensures that the virus will be contained in public meetings. The results of the sensitivity and specificity tests show that the goals have been met with an accuracy of 82.25 and 81.05 percent, respectively. According to the most recent findings of research, it may be possible for it to limit the spread of the virus by interfering with the chain-breaking mechanism when the virus is in the reproduction phase. The implementation of artificial intelligence (AI)-based contactless screening has proven to be an efficient method for preventing the spread of viruses in public gatherings and assisting various governments in their efforts to manage crowds. Another goal of this method is to aid in the management of crowds.

Data Availability

The data that support the findings of this study are available from the author on request.

Conflicts of Interest

The author declares that there are no conflicts of interest.

References

[1] D. S. Hui, T. A. Madani, F. Ntoumi et al., "The continuing 2019-nCoV epidemic threat of novel coronaviruses to global health—the latest 2019 novel coronavirus outbreak in Wuhan, China," *International Journal of Infectious Diseases*, vol. 91, pp. 264–266, 2020.

[2] E. Y. Ng, G. Kawb, and W. Chang, "Analysis of IR thermal imager for mass blind fever screening," *Microvascular Research*, vol. 68, no. 2, pp. 104–109, 2004.

[3] M.-F. Chiang, P. W. Lin, L. F. Lin et al., "Mass screening of suspected febrile patients with remote-sensing infrared thermography: alarm temperature and optimal distance," *Journal of the Formosan Medical Association*, vol. 107, no. 12, pp. 937–944, 2008.

[4] M. Condoluci, G. Araniti, T. Mahmoodi, and M. Dohler, "Enabling the IoT machine age with 5G: machine-type multicast services for innovative real-time applications," *IEEE Access*, vol. 4, pp. 5555–5569, 2016.

[5] F. Liu, D. Chen, X. Zhou, W. Dai, and F. Xu, "Let AI perform better next time—a systematic review of medical imaging-based automated diagnosis of COVID-19: 2020–2022," *Applied Sciences*, vol. 12, no. 8, p. 3895, 2022.

[6] P. Jain, W. F. Alsanie, D. O. Gago et al., "A cloud-based machine learning approach to reduce noise in ECG arrhythmias for smart healthcare services," *Computational Intelligence and Neuroscience*, vol. 2022, 2022.

[7] H. Kaushik, D. Singh, M. Kaur, H. Alshazly, A. Zaguia, and H. Hamam, "Diabetic retinopathy diagnosis from fundus images using stacked generalization of deep models," *IEEE Access*, vol. 9, Article ID 108276, 2021.

[8] Y. Pathak, P. K. Shukla, A. Tiwari, S. Stalin, and S. Singh, "Deep transfer learning based classification model for COVID-19 disease," *Irbm*, vol. 43, 2020.

[9] A. A. Bakhsh, A. Rizwan, A. B. Khoshaim, E. H. Abualsauod, and G. C. Altamirano, "Implications of COVID-19 on student learning satisfaction (sls): a remedial framework for universities," *International Journal of Engineering Education*, vol. 37, no. 6, pp. 1582–1593, 2021.

[10] E. Costan, G. Gonzales, R. Gonzales et al., "Education 4.0 in developing economies: a systematic literature review of implementation barriers and future research agenda," *Sustainability*, vol. 13, no. 22, Article ID 12763, 2021.

[11] A. Procházka, M. Schatz, O. Vysata, and M. Valis, "Microsoft kinect visual and depth sensors for breathing and heart rate analysis," *Sensors*, vol. 16, no. 7, p. 996, 2016.

[12] O. Gupta, D. McDuff, and R. Raskar, "Real-time physiological measurement and visualization using a synchronized multi-camera system," in *Proceedings of the IEEE Conference on Computer Vision and Pattern Recognition Workshops*, Las Vegas, NV, USA, June 2016.

[13] Y. Yan, X. Ma, L. Yao, and J. Ouyang, "Noncontact measurement of heart rate using facial video illuminated under natural light and signal weighted analysis," *Bio-Medical Materials and Engineering*, vol. 26, no. s1, pp. S903–S909, 2015.

[14] S. Goldberg, S. Heitner, F. Mimouni, L. Joseph, R. Bromiker, and E. Picard, "The influence of reducing fever on blood oxygen saturation in children," *European Journal of Pediatrics*, vol. 177, no. 1, pp. 95–99, 2018.

[15] R. Krishnamoorthi, S. Joshi, H. Z. Almarzouki et al., "A novel diabetes healthcare disease prediction framework using machine learning techniques," *Journal of Healthcare Engineering*, vol. 2022, 10 pages, 2022.

[16] G. Sun, T. Matsui, T. Kirimoto, and Y. Yao, "Applications of infrared thermography for noncontact and noninvasive mass screening of febrile international travelers at airport quarantine stations," in *Application of Infrared to Biomedical Sciences*Springer, Berlin, Germany, 2017.

[17] A. Martinez-Möller, D. Zikic, R. M. Botnar et al., "Dual cardiac–respiratory gated PET: implementation and results from a feasibility study," *European Journal of Nuclear Medicine and Molecular Imaging*, vol. 34, no. 9, pp. 1447–1454, 2007.

[18] X. Xiao, Z.-C. Wu, and K.-C. Chou, "A multi-label classifier for predicting the subcellular localization of gram-negative bacterial proteins with both single and multiple sites," *PLoS One*, vol. 6, no. 6, Article ID e20592, 2011.

[19] A. Basu, A. Routray, and R. Mukherjee, "Infrared imaging based hyperventilation monitoring through respiration rate estimation," *Infrared Physics & Technology*, vol. 77, pp. 382–390, 2016.

[20] H. Z. Almarzouki, H. Alsulami, A. Rizwan, M. S. Basingab, H. Bukhari, and M. Shabaz, "An internet of medical things-based model for real-time monitoring and averting stroke sensors," *Journal of Healthcare Engineering*, vol. 20219 pages, 2021.

[21] A. Motwani, P. K. Shukla, and M. Pawar, "Novel framework based on deep learning and cloud analytics for smart patient monitoring and recommendation (SPMR)," *Journal of Ambient Intelligence and Humanized Computing*, pp. 1–16, 2021.

[22] M.-Z. Poh, D. J. McDuff, and R. W. Picard, "Non-contact, automated cardiac pulse measurements using video imaging and blind source separation," *Optics Express*, vol. 18, no. 10, Article ID 10762, 2010.

[23] A. O. Al-Youbi, A. Al-Hayani, A. Rizwan, and H. Choudhry, "Implications of COVID-19 on the labor market of Saudi Arabia: the role of universities for a sustainable workforce," *Sustainability*, vol. 12, no. 17, p. 7090, 2020.